

MICROWAVE TRANSMISSION OF A HEXAGONAL ARRAY OF TRIANGULAR METAL PATCHES

G. Stevens, J. D. Edmunds, A. P. Hibbins, and J. R. Sambles*

Electromagnetic Materials Group, School of Physics, University of Exeter, EX4 4QL, UK

Abstract—The microwave transmission of hexagonal arrays consisting of patches of equilateral aluminium triangles has been experimentally studied as a function of metal occupancy (triangle size). As one would expect, at low frequencies the microwave transmission drops on passing through the connectivity threshold (50%) when the disconnected hexagonal array of metal triangles switches to a disconnected hexagonal array of equilateral holes. However, for higher frequencies resonant phenomena cause a complete reversal in this behaviour such that the transmission, on passing through the connectivity threshold, increases substantially.

1. INTRODUCTION

Since Ebbesen et al. [1] presented evidence of enhanced transmission of electromagnetic (EM) waves through a periodic array of sub-wavelength holes in a metal film there has been a substantial body of theoretical and experimental work on the subject. The majority of studies have centred on the manipulation of light on a sub-wavelength scale with artificial photonic structures [1–3] but there are also a significant number of publications concerning wavelengths beyond the visible [4–8].

Enhanced optical transmission (EOT) through these holey metal films was found [1] to be several orders of magnitude greater than the transmission predicted by Bethe's theory [9]. At visible frequencies, this EOT is generally attributed to the excitation of surface plasmons on either or both surfaces of the hole array [10, 11], which couple through the evanescent fields within the holes. The roles of the

Received 22 July 2011, Accepted 29 August 2011, Scheduled 7 September 2011

* Corresponding author: John Roy Sambles (j.r.sambles@exeter.ac.uk).

periodicity, film thickness and metal type have been elucidated both theoretically [2, 12] and experimentally [13–17].

At microwave frequencies there has been a large amount of work exploring the response of hole arrays (inductive meshes) as well as patch arrays (capacitive meshes) (see [18] and references therein), both of which are commonly referred to as frequency selective surfaces (FSSs) due to their behaviour in the long wavelength limit. Resonant behaviour may be observed when the incident wavelength λ_0 is approximately equal to twice one of the key dimensions in the structure. This may be expected to occur at wavelengths close to the typical hole or patch dimension (a patch resonance), or the periodicity of the structure (although when the wavelength reduces to that of the latter, then diffraction is likely to become important). Equivalent circuit theories [19–21] have been used to model such arrays, with inductive and capacitive elements determining the resonant frequency of the array and resistance determining the loss.

Recently [22] the relationship between metal occupancy of a square array of square patches and its microwave transmission has been investigated and it was found that on crossing the connectivity threshold, the magnitude of the transmitted signal actually increased rapidly for certain frequencies, as opposed to decreasing as one would perhaps naively expect. In this study the dependence of transmission as a function of metal occupancy of a hexagonal array of equilateral triangle metal patches is investigated. In a similar vein to the previous study [22] of squares in a square array, the geometry of this structure is also such that when the metal occupancy reaches 50% the triangles become connected and then a hexagonal array of equilateral triangular holes results, the complementary structure. (Such hexagonal arrays of holes are just the inverse of the metal patch structure at the equivalent lower occupancy, and their response function for the orthogonal incident polarisation may be predicted using Babinet's theorem [23].) This equilateral triangle geometry along with the square patch geometry are those with the highest symmetry with this property. Other patch shapes may be considered but the triangular shape is that with the highest symmetry leading to the smallest azimuthal angle dependence, further it and the square array are the two highest symmetry states with complete Babinet self-complementarity. Crucially, like the square patch array, this triangle structure also enables the dependence of the microwave transmission on the metal occupancy either side of the connectivity threshold (when the metal patches switch from disconnected to connected) to be fully explored. Conventional wisdom would have it that the high microwave transmission of a regular array of triangular metal

patches will switch off on increase of the metal occupancy through the connectivity threshold. However, the results presented here show that, for frequencies close to the diffraction edge, the existence of a resonance causes the microwave transmittance to go from zero to close to unity through this threshold — a complete reversal of the expected behaviour at lower frequencies.

2. RESULTS

Samples were produced using a hexagonal array geometry having centre to centre distance $d = 6.00$ mm (minimum lattice spacing $d' = 5.196$ mm with an equilateral triangle patch of side length a on each lattice point (Figure 1).

The samples were produced using conventional photolithographic and chemical etching techniques to pattern a nominally 60 nm thick aluminium layer on a 75 μm Mylar® substrate. Despite the thickness of the aluminium layer being much less than the skin depth for the frequency range studied (~ 1 μm), it is essentially completely opaque to microwaves due to its Drude-like dielectric function, $\text{Im}(\varepsilon) \rightarrow \infty$, manifested as a large impedance mismatch. Samples were fabricated to cover the range of occupancies, X , from no metal to continuous aluminium ($0 \leq X \leq 100\%$) by varying the side length of the patches a . For all samples with $a > 6.00$ mm the patches become connected forming the inverse structure, a conducting mesh network: a triangular hole array.

Each sample is supported on a 3 mm thick sheet of expanded polystyrene, having a refractive index ~ 1 at these frequencies, and is placed behind a 100 mm \times 100 mm aperture formed from microwave

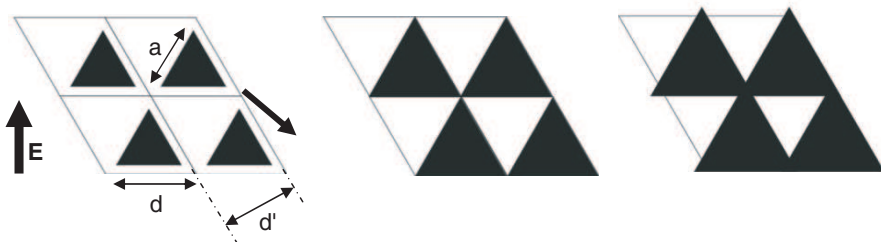


Figure 1. Diagram illustrating the increase of metal patch size with constant pitch to form a fully conducting network (array of equilateral holes). Black denotes the aluminium and the lines indicate four unit cells making the array. \mathbf{E} denotes the orientation of the electric vector of the incident microwaves.

absorbing material. A collimated microwave beam is incident normal to the sample and transmission measurements, normalised to transmission through the aperture and polystyrene sheet without a sample, are taken in the frequency range 26.5 to 60 GHz. First order diffraction for normal incidence radiation occurs at 57.7 GHz due to the grating periodicity $d' = 5.196$ mm. Typical results are shown in Figure 2.

Modelling of the expected electromagnetic response was undertaken using a finite element method (FEM) model [24] with the unit cell illustrated in Figure 1, with periodic boundary conditions. The sample was therefore assumed infinite in the xy -plane and the incident wave was modelled as a perfect plane wave. However, in reality, the sample and beam spot are both finite and there is also a small incident angle spread of $\sim 1.5^\circ$. The metal patches were also modelled as having zero thickness and as perfect electrical conductors. Whilst this is an often used approximation in the microwave regime it does lead to small discrepancies between the experimental and modelled data, primarily in the absolute amplitude of the response rather than the frequencies at which specific features occur.

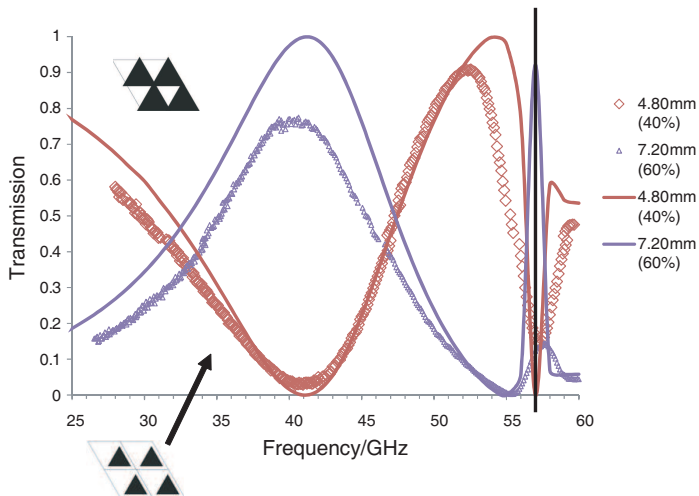


Figure 2. Transmission (normalised to perfect transmission of 1) measurements for two patch sizes of a hexagonal array of pitch 6.00 mm with normal incidence radiation and the electric field vector polarised perpendicular to the base of the triangles. The schematic sketches of the sample illustrate its connectivity, modelled data is represented as a continuous line and the solid vertical line marks the diffraction edge.

The comparison between the experimental data and the model predictions can be improved by the introduction of a finite thickness and loss of the metal. However such modelling is computationally intensive and therefore time consuming. In any case it is clear that one can fully interpret the results without this added complexity.

The disconnected arrays exhibit the low-pass frequency filtering commonly found for a regular capacitive patch array [18] as there is no continuous metallic pathway available for the currents to flow around the system. Conversely, the connected arrays exhibit high-pass frequency filtering which is expected with inductive meshes [11] as now the currents are able to propagate through the continuous array of metal. A sample with a given metal occupancy ($X\%$) is the inverse of a sample with occupancy of $(100 - X\%)$. By applying Babinet's principle [23] and considering the sample to be of zero thickness and to be a perfect conductor, a sample with $X\%$ occupancy will have a normal incidence transmission T_x , while the $(100 - X\%)$ sample will have a transmission of $(1 - T_x)$. (Note that strictly the polarisation needs to be rotated by 90° but for these high symmetry samples the normal incidence transmission response is the same as at 0° .)

Figure 2 demonstrates this to a substantial degree, as for example at about 41 GHz the 60% sample has a minimum in transmission whereas the 40% sample has a maximum. It is apparent however that the two responses do not sum to 1 as would be expected as there is between a 10 and 20% absorption loss in the sample (not accounted for in the model).

Each sample exhibits a transmission resonance near to but below the diffraction edge which takes the form of a sharp minimum (Figure 3(a)) for the disconnected samples ($a < 6.00$ mm) and a sharp maximum (Figure 3(b)) for the connected samples ($a > 6.00$ mm). For occupancies below 50% there are clearly two minima which become broader and shift down in frequency as the occupancy is increased towards 50%. For the triangular-hole samples with occupancy above 50% (Figure 3(b)), the two maxima likewise become broader and move down in frequency as the occupancy is decreased towards 50%. For 50% there are two degenerate solutions (50% is of course a singularity) and in Figure 3(a) we show the solution for just below 50% while in Figure 3(b) is shown the solution for just above 50%. They are the expected inverse of each other. Figure 4 shows the electric field plots for the metal patch sample with $a = 4.80$ mm ($X = 40\%$), solved at the frequencies of the two minima (41 and 57 GHz). These show that for the 41 GHz (Figure 4(a)) mode there are three strong regions of electric fields at the corners of the patches (three nulls at the centre of the edges) while for the 57 GHz mode (Figure 4(b)) there are six

regions of strong electric field with three at the centre of the edges as well as three at the corners (two nulls per edge). Electric field plots from FEM modelling of the complimentary structure ($X = 60\%$) are also shown in Figure 4. The mode at 41 GHz (Figure 4(c)) now has

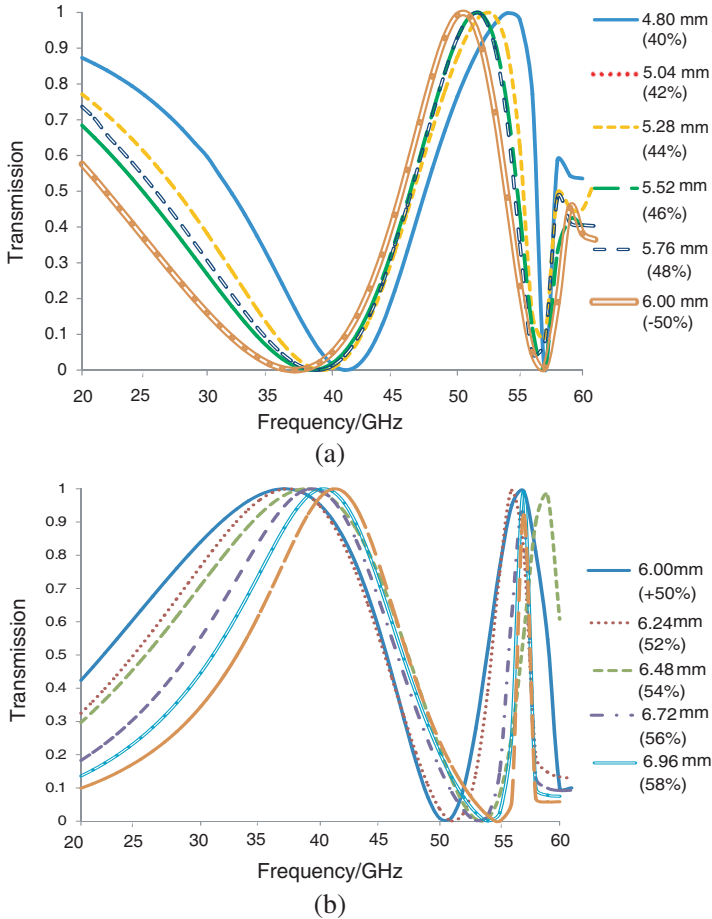


Figure 3. (a) Model transmission (normalised to perfect transmission of 1) for arrays of pitch $d = 6.00$ mm with occupancy $40\% \leq X \leq 50\%$ for normal incidence and electric field vector polarised perpendicular to base of triangles. (b) Model transmission (normalised to perfect transmission of 1) for arrays of pitch $d = 6.00$ mm with occupancy $50\% \leq X \leq 60\%$ for normal incidence and electric field vector polarised perpendicular to base of triangles. (Models undertaken with Ansoft's HFSS finite element package [24].)

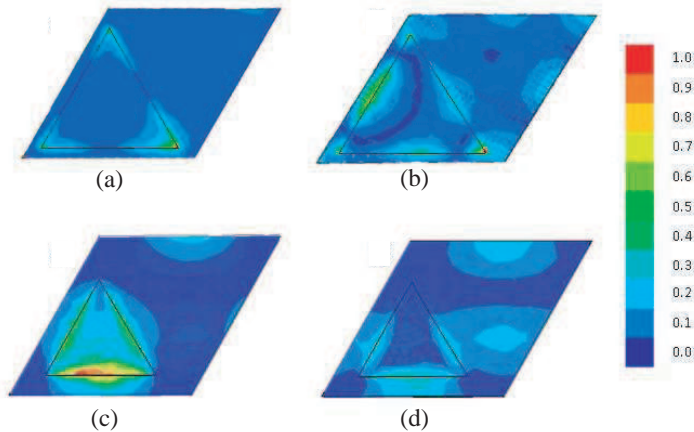


Figure 4. Electric fields (arbitrary units) from FEM modelling of a unit cell for $a = 4.80$ mm ($X = 40\%$) samples at (a) $\nu = 41.0$ GHz and (b) $\nu = 57.0$ GHz. Also shown are the electric field plots for the complimentary structure $a = 7.20$ mm ($X = 60\%$) samples at (c) $\nu = 41.0$ GHz (d) $\nu = 57.0$ GHz. (Models fields computed using Ansoft's HFSS finite element package [24].)

strong electric fields along the edges of the holes and three nulls at the corners and is complimentary to the patch resonance of Figure 4(a). The second mode at 57 GHz (Figure 4(d)) does not appear to simply relate to that on the complementary metal patch structure and from the field plots it is seen that the magnetic fields from adjacent holes are connected and the transmission enhancement may be associated with propagating currents. These two higher frequency modes at 57 GHz are affected by the evanescent diffraction and as such are much less localised on the patches or within separate holes respectively.

Figure 5 shows the transmission as a function of occupancy for a selection of fixed frequencies. For very low frequencies the transition at 50 % occupancy would be expected to be a step from full transmission to zero transmission. However, Figure 5 shows that this is clearly not the case. At 25.0 GHz the transmission behaviour upon passing through 50% occupancy gives the inverse character and results in a 20% increase in transmission. As the frequency is further increased the transmission increase on passing through the connectivity threshold becomes larger except for at 45 and 50 GHz where the transmission drops suddenly on going through the connectivity threshold due to the resonant mode for $45\% < X < 50\%$ samples occurring just

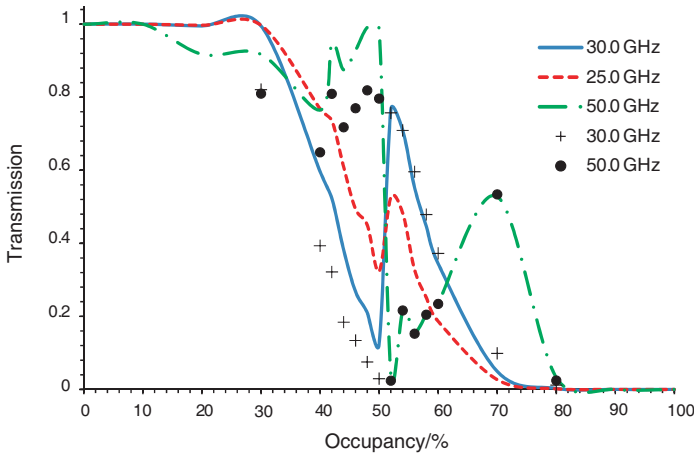


Figure 5. Normal incidence transmission (normalised to perfect transmission of 1) as a function of metal occupancy for a hexagonal array of equilateral triangular patches. Data are shown as symbols while the models, for a PEC metal, are shown as lines.

before the connectivity threshold at these frequencies. Above 55 GHz the transmission again increases dramatically on passing through the connectivity threshold.

This inverted behaviour is clearly associated with the resonance exhibited by each sample near to the diffraction edge. This resonance is seen in Figure 2 as a **minimum** in transmission for the disconnected samples and a **maximum** in transmission for the connected patch samples. These resonances are a hybridisation of the evanescent diffraction from the periodicity of the array with the resonant mode of each patch/hole. The strength of the evanescent diffracted orders is greatest closest to the onset of the first propagating diffracted order and it is at these frequencies that the inversion effect is most apparent. There are also two transmission channels present: a resonant and a non-resonant contribution and interference between these two channels that leads to the characteristic Fano-resonance shape.

3. CONCLUSIONS

An original study of the affect on microwave transmission of the metal occupancy of a hexagonal array of aluminium patches of equilateral triangles has been presented. For frequencies well below the diffraction edge there exist strong resonant modes which are associated largely

with individual elements of the structures (either patches or holes). For frequencies approaching the diffraction edge the response is now more complex being a mixture of the response of individual elements (patches or holes) coupled via evanescent diffraction fields leading to unusual transmission characteristics of the structures. In particular the expected decrease in transmission on passing through the connectivity threshold (50% occupancy) may now be reversed due to the presence of these spatially extended resonant modes, producing an unexpected large increase in transmission at frequencies somewhat below the diffraction edge where the evanescent diffractive fields play a key role. The results found accord well with those predicted from finite element modelling using a perfect electrical conductor approximation with the caveat that in reality finite conductance of the metal leads to some absorption loss. Highly symmetric patch arrays of the type studied here and also in reference 22 provide incidence angle independent selective filters (Salisbury screens) but possibly more significantly when used near the connectivity threshold with a small measure of disorder they give the opportunity for broad band 50% mirrors. Further because of the inverse character of the resonance they provide a new type of structure to add to the already wide palette of patterned metal structures for controlling microwaves.

ACKNOWLEDGMENT

GS is grateful to ESPRC for financial support through the summer bursary scheme.

REFERENCES

1. Ebbesen, T. W., H. J. Lezec, H. F. Ghaemi, T. Thio, and P. A. Wolff, "Extraordinary optical transmission through sub-wavelength hole arrays," *Nature*, Vol. 391, 667, 1998.
2. Martin-Moreno, L., F. J. García-Vidal, H. J. Lezec, K. M. Pellerin, T. Thio, J. B. Pendry, and T. W. Ebbesen, "Theory of extraordinary optical transmission through subwavelength hole arrays," *Phys. Rev. Lett.*, Vol. 86, 1114, 2001.
3. Genet, C. and T. W. Ebbesen, "Light in tiny holes," *Nature*, Vol. 445, 39, 2007.
4. Antonets, I. V., L. N. Kotov, S. V. Nekipelov, and E. N. Karpushov, "Conducting and reflecting properties of thin metal films," *Tech. Phys.*, Vol. 49, 1496, 2004.

5. Kelly, R. J., M. J. Lockyear, J. R. Suckling, J. R. Sambles, and C. R. Lawrence, "Enhanced microwave transmission through a patterned metal film," *Appl. Phys. Lett.*, Vol. 90, 223506, 2007.
6. Hansen, R. C. and W. T. Pawlewicz, "Effective conductivity and microwave reflectivity of thin metallic films," *IEEE Trans. Microw. Theory Tech.*, Vol. 30, 2064, 1982.
7. Lagarkov, A. N., K. N. Rozanov, A. K. Sarychev, and N. A. Simona, "Experimental and theoretical study of metal-dielectric percolating films at microwaves," *Physica A*, Vol. 241, 199, 1997.
8. Kim, J. H. and P. J. Moyer, "Transmission characteristics of metallic equilateral triangular nanohole arrays," *Appl. Phys. Lett.*, Vol. 89, 121106, 2006.
9. Bethe, H. A., "Theory of diffraction by small holes," *Phys. Rev.*, Vol. 66, 163, 1944.
10. Ghaemi, H. F., T. Thio, D. E. Grupp, T. W. Ebbesen, and H. J. Lezec, "Surface plasmons enhance optical transmission through subwavelength holes," *Phys. Rev. B*, Vol. 58, 6779, 1998.
11. Popov, E., M. Neviere, S. Enoch, and R. Reinisch, "Theory of light transmission through subwavelength periodic hole arrays," *Phys. Rev. B*, Vol. 62, 16100, 2000.
12. Popov, E., S. Enoch, G. Tayeb, M. Neviere, B. Gralak, and N. Bonod, "Enhanced transmission due to nonplasmon resonances in one- and two-dimensional gratings," *Appl. Opt.*, Vol. 43, 999, 2004.
13. Avrutsky, I., Y. Zhao, and V. Kochergin, "Surface-plasmon-assisted resonant tunneling of light through a periodically corrugated thin metal film," *Opt. Lett.*, Vol. 25, 595, 2000.
14. Grupp, D. E., H. J. Lezec, T. W. Ebbesen, K. M. Pellerin, and T. Thio, "Fundamental role of metal surface in enhanced transmission through subwavelength apertures," *Appl. Phys. Lett.*, Vol. 77, 1569, 2000.
15. Thio, T., H. F. Ghaemi, H. J. Lezec, P. A. Wolff, and T. W. Ebbesen, "Surface-plasmon-enhanced transmission through hole arrays in Cr films," *Opt. Soc. Am. B*, Vol. 16, 1743, 1999.
16. Degiron, A., H. J. Lezec, W. L. Barnes, and T. W. Ebbesen, "Effect of hole depth on enhanced light transmission through subwavelength hole arrays," *Appl. Phys. Lett.*, Vol. 81, 4327, 2002.
17. Papasimakis, N., V. A. Fedotov, A. S. Schwanecke, N. I. Zheludev, and F. J. Garcia de Abajo, "Enhanced microwave transmission through quasicrystal hole arrays," *Appl. Phys. Lett.*, Vol. 91, 081503, 2007.

18. Munk, B. A., *Frequency Selective Surfaces: Theory and Design*, Wiley, New York, 2000.
19. Ulrich, R., "Far-infrared properties of metallic mesh and its complementary structure," *Infrared Phys.*, Vol. 7, 37, 1967.
20. Whitbourn, L. B. and R. C. Compton, "Equivalent-circuit formulas for metal grid reflectors at a dielectric boundary," *Appl. Opt.*, Vol. 24, 217, 1985.
21. Dawes, D. H., M. C. McPhedran, and L. B. Whitbourn, "Thin capacitive meshes on a dielectric boundary: Theory and experiment," *Appl. Opt.*, Vol. 28, 3498, 1989.
22. Edmunds, J. D., A. P. Hibbins, J. R. Sambles, and I. J. Youngs, "Resonantly inverted microwave transmissivity threshold of metal grids," *New Journal of Physics*, Vol. 12, 063007, 2010.
23. Babinet, M., "Mémoires d'optique météorologique," *Comptes Rendus de l'Académie des Sciences*, Vol. 4, 638, 1837.
24. Finite Element Modelling: HFSSTM, Ansoft Corporation, Pittsburgh, CA, USA.